Iron-based layered compound LaFeAsO is an antiferromagnetic semimetal

Fengjie Ma[1] and Zhong-Yi Lu[2,*]
[1]*Institute of Theoretical Physics, Chinese Academy of Sciences, Beijing 100080, People's Republic of China*
[2]*Department of Physics, Renmin University of China, Beijing 100872, People's Republic of China*
(Received 10 June 2008; published 30 July 2008)

LaFeAsO is a parent compound of iron-based F-doped superconductors. An understanding of its ground phase and electronic structure is a precondition to understanding the underlying superconductivity mechanism. Our study shows that LaFeAsO is a quasi-two-dimensional antiferromagnetic semimetal with most carriers being electrons and with a magnetic moment of $2.3\mu_B$ located around each Fe atom on the Fe-Fe square lattice. Physically, this is a commensurate antiferromagnetic spin-density wave due to the Fermi-surface nesting. The observed superconduction after the F doping happens on the Fe-Fe layer suggesting a new superconductivity mechanism mediated by spin fluctuations.

DOI: 10.1103/PhysRevB.78.033111 PACS number(s): 74.25.Jb, 71.18.+y, 74.25.Ha, 74.70.−b

Just recently an iron-based layered compound LaFeAsO was reported to show superconductivity after doping F atoms to replace O atoms at a concentration of 3–13 atom%, with the highest critical temperature of about 26 K.[1] In comparison with those high T_c oxide superconductors in which superconduction happens on CuO_2 layers,[2] the LaFeAsO possesses conduction and further superconduction at iron-based FeAs layers. This strongly suggests that there would be a new superconductivity mechanism because unlike the case of superconduction at CuO_2 layers it is the Fe atoms that directly play an important role, in which there would be many interactions and degrees involved, such as electronic and magnetic.

It is well known that for the high T_c oxide superconductors verifying the ground phase of the parent compound La_2CuO_4 as an antiferromagnetic (AFM) insulator is essential to studying the high T_c superconductivity mechanism. Similarly, to clarify the ground phase of LaFeAsO and to further understand its electronic and magnetic structure are the keys to start understanding the new possible superconductivity mechanism. We have performed the first-principles electronic structure calculations, with the target of understanding LaFeAsO.

It has also been known that at low temperatures in line with $3d$ transition metals in their element form, Cr and Mn usually take antiferromagnetic state while Co and Ni are ferromagnetic. The in-between Fe displays a variety of magnetic phases, for example, bcc-Fe is a strong ferromagnet, but fcc-Fe may be nonmagnetic, ferromagnetic, antiferromagnetic, or even spin-density wave dependent on the local environment.[3] It is thus expected that the Fe atoms show novelty in the LaFeAsO compound. Indeed our studies show a very interesting finding: The compound LaFeAsO is an antiferromagnetic semimetal rather than a nonmagnetic metal. Furthermore this is a quasi-two-dimensional commensurate spin-density wave, due to the Fermi-surface nesting.

We notice that there have now been a number of theoretical or calculated works on this very important issue.[4–6] All of these authors claim that the compound LaFeAsO is a nonmagnetic metal. In fact, our calculations show that the nonmagnetic state is metastable. There is a barrier between the antiferromagnetic state and the nonmagnetic state in the electronic degree configurations. Clearly they found a local minimum (nonmagnetic state) but missed a global minimum (antiferromagnetic state).

We carried out the first-principles calculations by using the plane-wave basis method.[7] We adopted the local-(spin)-density [L(S)DA] approximation and the generalized gradient approximation (GGA) of Perdew-Burke-Ernzerhof (PBE) (Ref. 8) for the exchange-correlation potentials. Also, the ultrasoft pseudopotentials[9] were used to model the electron-ion interactions. After the full convergence test, the kinetic-energy cutoff and the charge-density cutoff of the plane-wave basis were chosen to be 800 and 6400 eV, respectively. The Gaussian broadening technique was used and a mesh of $36\times36\times18$ k points were sampled for the Brillouin-zone integration. For all relaxed structures, the convergence sets by the forces being smaller than 0.01 eV/Å.

The parent compound LaFeAsO crystallizes in a tetragonal layered structure, being a member of quaternary oxypnictide family LaOMPn (M=Cr, Mn, Fe, Co, and Ni and Pn=P and As). Its unit cell, also adopted as the calculation cell, consists of two formula subunits with eight atoms limited to the symmetry of $P4/nmm$ space group, in which FeAs layers and LaO layers are arranged, alternating along the c axis. In the calculations, the experimental lattice parameters a=4.035 52 Å, c=8.7393 Å were adopted while the two internal coordinates of La and As atoms within the cell were determined by the energy minimization. We emphasize that the Fe atoms form a two-dimensional square lattice with a separation of 2.85 Å. Towards the end, we checked the lattice parameters by the energy minimization, and found less than 1% change, so there are no meaningful changes in the results.

We first studied the nonmagnetic (NM) state of the compound LaFeAsO, which means that spin degrees were not included in the calculation. Such a study provides a reference for investigating magnetization states, by which we can better understand the mechanism underlying the magnetization, if existing. Our calculated results on the NM state are similar to those in Refs. 4–6. From Fig. 1(a), we see that the density of states (DOS) may be divided into two parts: The lower part (2 eV below the Fermi energy) consists of those bands formed through the bonding between O and La atomic orbitals and Fe and As atomic orbitals, and the upper part consists basically of the Fe $3d$ orbital bands ranging from −2 eV to 2

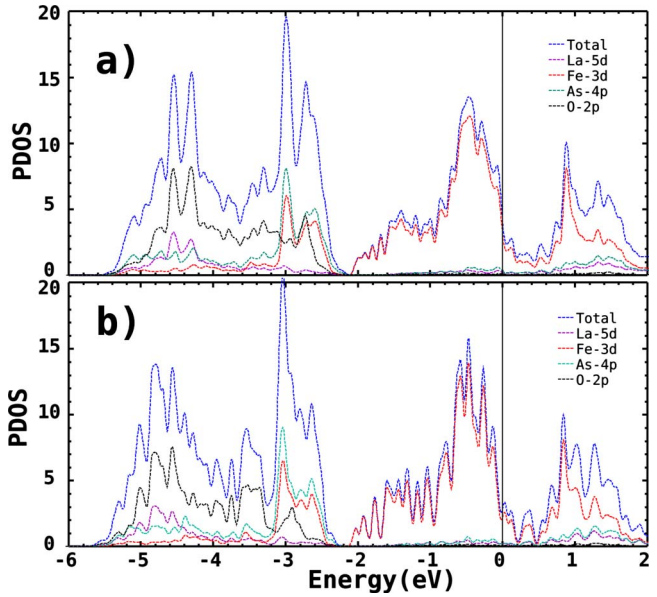

FIG. 1. (Color online) Calculated atomic orbital-resolved partial density of states of $LaO_{1-x}F_xFeAs$ in nonmagnetic state. (a) Parent compound LaFeAsO; (b) $LaO_{0.95}F_{0.05}FeAs$ (5% F doping). The Fermi energy sets to zero.

eV centered at the Fermi energy. Further analysis of the calculation shows that the crystal-field effect upon the Fe 3*d* orbitals is much weaker than in transition metal oxides. This is because the electronegativity of As is much smaller than that of O. Thus all Fe 3*d* electrons are expected to play a dominant role in conduction and related superconductivity if LaFeAsO is nonmagnetic.

Figure 2(b) shows that the Fermi surface is made up of five sheets derived from the five bands crossing the Fermi energy marked by numbers in Fig. 2(a). Among these five sheets, the two sheets due to two electron bands marked by 4 and 5 are forming two cylinderlike shapes centered around *M*-*A*, and the other three due to three hole bands marked by 1, 2, and 3 are forming two cylinderlike shapes centered around Γ-*Z* and one pocket around *Z*, respectively. As we see, because of nearly no band dispersion along (001), the conduction is strongly anisotropic, only happening on the

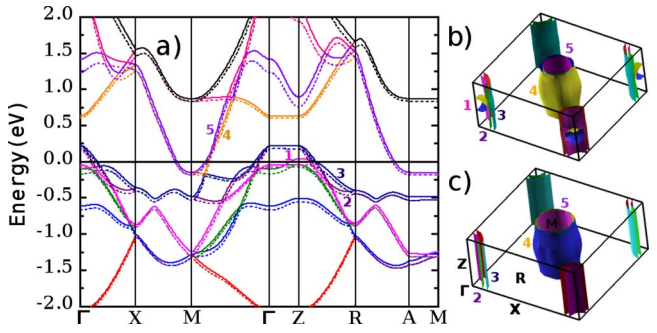

FIG. 2. (Color online) Calculated nonmagnetic electronic structures of $LaO_{1-x}F_xFeAs$. (a) Energy-band structures: the solid lines for the undoping while the dotted lines for the 5% F doping (the Fermi energy sets to zero); (b) undoping: Fermi surface; (c) 5% F doping: Fermi surface.

FeAs layers. The volumes enclosed by these Fermi sheets give 0.28 electrons/cell and equally 0.28 holes/cell, namely, $1.97\times10^{21}/\mathrm{cm}^3$. The compound LaFeAsO in the NM state is thus a semimetal with a low carrier density between normal metals and semiconductors.

The F-doping effects on the electronic structures of $LaO_{1-x}F_xFeAs$ were studied at $x=3\%$, 5%, 8%, 10%, and 15% by using virtual crystal calculations. Figure 2(a) shows that the 5% F doping just relatively moves the Fermi level slightly up, i.e., increasing the number of electrons while reducing the number of holes in the unit cell. This is also clearly shown by changes in the Fermi surface shown in Fig. 2(c), in which the hole pocket disappears and the two hole cylinders shrink while the two electron cylinders expand obviously. Such a change is found up to the 15% F doping. Thus the F-doping effect can basically be considered as doping electrons. On the other hand, Fig. 1(b) shows that the density of states at the Fermi energy heavily decreases with the F doping, which suggests that the doping in the NM state may not favor the superconductivity even though the total electron carrier density increases. The doping also introduces more wiggles in the DOS [Fig. 1(b)].

We next included spin degrees to study magnetization states of the compound LaFeAsO. Here we define the spin-density polarization as the ratio of the difference to the sum, between the charge densities with spin up and spin down. We first broke the spin-up and spin-down symmetry by assigning ferromagnetic moments to the Fe atoms. It turns out that no matter how large the assigned initial moments are, the system always evolves into a NM state without any local moment remaining, namely, back to the initial NM state. LaFeAsO will thus not display ferromagnetic behavior. We then assigned AFM moments to the two Fe atoms in the unit cell to break the spin-up and spin-down symmetry. We find that when the initial AFM assignment with the spin-density polarization is set less than 6%, the system still evolves back into the NM state. However, when the spin-density polarization is set larger than 6%, the system evolves into a stable AFM state with the energy lowered by 0.16 eV/cell. The internal coordinates of As and La in the unit cell can be further relaxed, which lowers the energy by extra 0.06 eV/cell. Eventually this AFM state is more stable in energy by 0.22 eV/cell than the NM state. Finally about a $2.38\mu_B$ magnetic moment is formed around each Fe atom. We have thus shown that there exist two stable states, namely, the NM state and the AFM state, in electronic degree configurations for the compound LaFeAsO. Between the two states, the AFM state is more favorable in energy to be the ground state and the NM state is then to be a metastable state. We also did the independent calculation by using the full potential linearized augmented plane-wave (FLAPW) method with the code WIEN2K package,[10] which also indicates that the LaFeAsO ground state is antiferromagnetic.

In comparison to the NM state (Fig. 2), there are now just three bands crossing the Fermi energy (Fig. 3); the previous bands 1 and 2 in Fig. 2(a) are now pushed down further, making the hole pocket and one hole cylinder disappear in the AFM state. Meanwhile, the bands 4 and 5 in Fig. 2(a) nearly emerging around *M* and *A* are now splitting, in which the band 4 is going down while the band 5 is going up in the

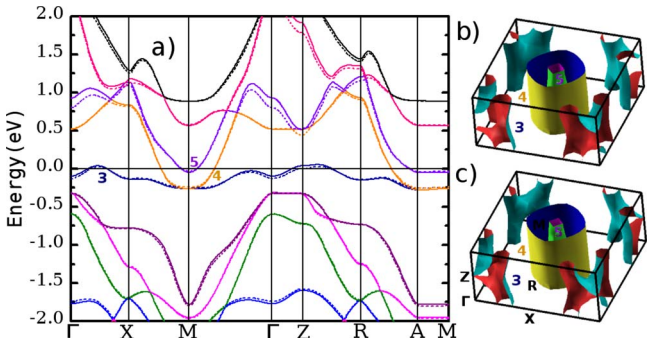

FIG. 3. (Color online) Calculated antiferromagnetic electronic structures of $LaO_{1-x}F_xFeAs$. (a) Energy-band structures: the solid lines for the undoping while the dotted lines for 5% F doping (the Fermi energy sets to zero); (b) undoping: Fermi surface; (c) 5% F doping: Fermi surface. Note that here only the spin-up part is shown.

AFM state. These changes in the energy-band structure overall make the AFM state more favorable in energy. This can apparently be attributed to the exchange energy lowering. However, when we compare the Fermi surfaces between the NM [Fig. 2(b)] and the AFM [Fig. 3(b)] states, we find that there exists the Fermi-surface nesting in the NM Fermi surface that may induce the AFM Fermi surface, as shown in Fig. 4(a). The nesting vector is $\vec{Q}=(\frac{\pi}{a},\frac{\pi}{a},0)$ between the hole sheets and the electron sheets. Figure 5 plots the calculated AFM spin-polarized charge-density distribution in the LaFeAsO unit cell, which indicates that the AFM state is a quasi-two-dimensional spin-density wave, oscillating as $\vec{M}\cos(\vec{Q}\cdot\vec{R})$ on the Fe-Fe square lattice with a wave vector equal to the nesting vector $\vec{Q}$ [(π,π) or $(\pi,-\pi)$] ($\vec{R}$ the lattice site vector). We thus conclude that the underlying physics to stabilize the AFM state is the Fermi-surface nesting. It turns out that the AFM electronic structure is quite different from the NM one, especially around the Fermi energy.

From the calculated AFM density of states shown in Fig. 7, we see that a gap opens around −0.5 eV in contrast to the NM state in Fig. 1(a) because of the Fermi-surface nesting. This is also reflected between the band structures of the NM and AFM states [Fig. 2(a) and Fig. 3(a)]. Corresponding to this opening, more states are pushed down to around −2.0 eV. Meanwhile, the density of states at the Fermi energy becomes larger [Fig. 7(a)], being nearly double (spin up plus down) of that in the NM case [Fig. 1(a)]. The projected density of states in Fig. 6 further shows that there is basically

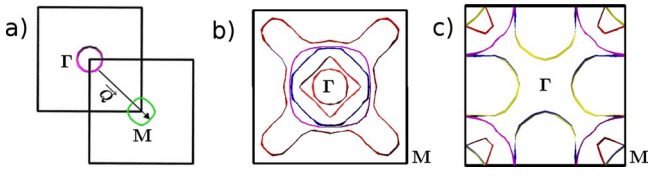

FIG. 4. (Color online) Calculated nonmagnetic Fermi-surface cross sections through Γ and M in the (001) plane. (a) LaFeAsO: The nesting vector is denoted by $\vec{Q}=(\frac{\pi}{a},\frac{\pi}{a},0)$, between Γ and M, with a being the lattice constant; (b) LaMnAsO; (c) LaCoAsO.

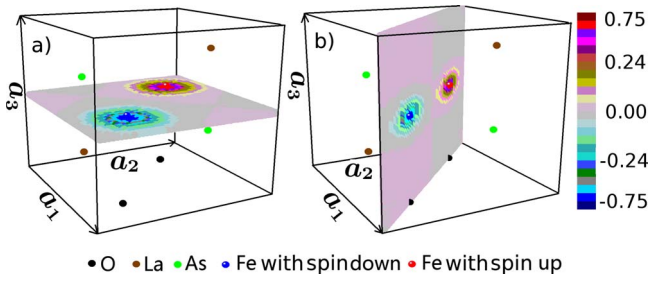

FIG. 5. (Color online) Calculated antiferromagnetic spin-polarized charge-density distribution in the LaFeAsO unit cell: (a) in the Fe-Fe square lattice plane; (b) perpendicular to the Fe-Fe square lattice plane. Here the dark (red) part denotes spin up and the gray (blue) part denotes spin down.

no contribution from the Fe-$3d_{x^2-y^2}$ orbitals between −0.6 eV and 0.6 eV centered at the Fermi energy while the Fe-$3d_{z^2}$ with $3d_{xz}$, $3d_{yz}$, and $3d_{xy}$ are dominant in this range. Physically this is because the Fe-$3d_{x^2-y^2}$ orbitals have formed a very strong bond along the nearest Fe-Fe direction that the derived band is very below the Fermi energy. Further inspection of the calculations shows that the hole portion in Fig. 3(b) consists mostly of the Fe-$3d_{z^2}$ orbitals with a very small portion of As-$4p_z$ orbitals, while the two electron cylinders consist of the Fe $3d_{xz}$, $3d_{yz}$, and $3d_{xy}$ orbitals. Moreover, in the AFM state, the volumes enclosed by the Fermi-surface sheets in Fig. 3(b) yield 0.26 electrons/cell ($1.83\times10^{21}/\mathrm{cm}^3$) and 0.12 holes/cell ($0.84\times10^{21}/\mathrm{cm}^3$), respectively. Thus the parent compound LaFeAsO is an AFM semimetal, with most carriers being electrons. Note that in the NM state, the carrier densities of electrons and holes are equal. Thus we predict that there will be an abrupt change in the Hall measurement for the compound LaFeAsO from high temperatures to low temperatures, corresponding to the transition from the NM phase to the AFM phase.

We also undertook further calculations to check how stable this AFM state is under the F doping. Similar to the NM case [Fig. 2(a)], Fig. 3(a) shows that the 5% F doping is also just rigidly moving the Fermi level slightly up, increasing the number of electrons while decreasing the number of holes in the unit cell. The volume enclosed by hole Fermi-surface sheet number 3 shrinks obviously in Fig. 3(c). We

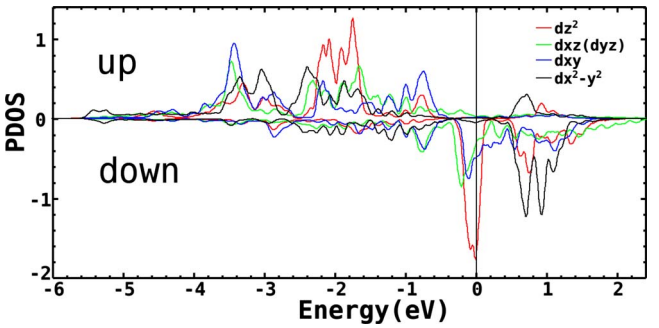

FIG. 6. (Color online) Calculated antiferromagnetic density of states projected into the Fe-$3d$ atomic orbitals around one of the two Fe atoms in the unit cell. Note that the spin up and the spin down are reversed around the other Fe atom.

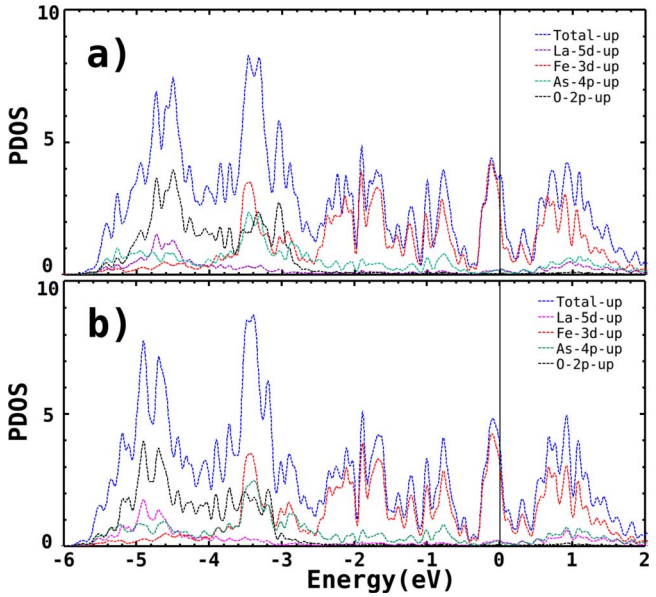

FIG. 7. (Color online) Calculated atomic orbital-resolved partial density of states of the compound $LaO_{1-x}F_xFeAs$ in antiferromagnetic state. The Fermi energy sets to zero. (a) Parent compound LaFeAsO; (b) $LaO_{0.95}F_{0.05}FeAs$ (5% F doping). Note that here only the spin-up part is shown.

find that such a change in the electronic structure is taken until the 15% F doping with negligible effect on the AFM spin-density wave. Thus the AFM state is stable against the F doping. The F-doping effect on the AFM phase is also basically to dope electrons. Unlike in the NM state, the density of states at the Fermi energy now decreases very little with doping [Fig. 7(b)].

We notice that the superconductivity takes place in the experiment when the F-doping concentration is between 3% and 13%,[1] in which the concentration range of the compound $LaO_{1-x}F_xFeAs$ in normal phase will hold the AFM spin-density wave according to our calculations. Further the itinerant Fe $3d$ electrons are also dominant around the Fermi surfaces, so the superconductivity continues working on the AFM layers with the electron pairing, which we suggest to be mediated by the spin fluctuations.

We also carried out the calculations in order to search for the trend in line with M=Cr, Mn, Fe, Co, and Ni in LaOMAs and LaOMP. The calculated results on LaOMAs are similar to those reported in Ref. 5, except for LaFeAsO that has just been reported and analyzed in this Brief Report. The scrutiny of the Fermi-surface structures further evinces that there is no more Fermi-surface nesting, or at least no commensurate nesting, as shown in Figs. 4(b) and 4(c). The Fermi-surface nesting only happens on LaFeAsO, being an underlying mechanism to stabilize its AFM, which makes LaFeAsO distinct from the others in the line.

In conclusion, our studies indicate that the iron-based layered LaFeAsO as a parent compound of the F-doped superconductors is a quasi-two-dimensional antiferromagnetic semimetal, in which the antiferromagnetic spin-density wave forms on the Fe-Fe square lattice due to the Fermi-surface nesting. This antiferromagnetic state is robust against the F doping. This provides a new platform on which the superconductivity takes place after F doping, strongly implying a new underlying superconductivity mechanism.

We wish to thank Tao Xiang for stimulating and helpful discussions and N. L. Wang and J. L. Luo for helpful conversations. The computing resources were provided by Super-Computing Center and Institute of Theoretical Physics, Chinese Academy of Sciences. This work was supported by National Natural Science Foundation of China (Grant No. 10725419) and by National Basic Research Program of China (Grant No. 2007CB925004).

*zlu@ruc.edu.cn

[1] Y. Kamihara, T. Watanabe, M. Hirano, and H. Hosono, J. Am. Chem. Soc. **130**, 3296 (2008).
[2] J. D. Bednorz and K. A. Muller, Z. Phys. B: Condens. Matter **64**, 189 (1986); M. K. Wu, J. R. Ashburn, C. J. Torng, P. H. Hor, R. L. Meng, L. Gao, Z. J. Huang, Y. Q. Wang, and C. W. Chu, Phys. Rev. Lett. **58**, 908 (1987).
[3] V. L. Moruzzi, P. M. Marcus, K. Schwarz, and P. Mohn, Phys. Rev. B **34**, 1784 (1986); C. S. Wang, B. M. Klein, and H. Krakauer, Phys. Rev. Lett. **54**, 1852 (1985); M. Korling and J. Ergon, Phys. Rev. B **54**, R8293 (1996); Y. M. Zhou, D. S. Wang, and Y. Kawazoe, *ibid.* **59**, 8387 (1999).
[4] D. J. Singh and M. H. Du, Phys. Rev. Lett. **100**, 237003 (2008).
[5] G. Xu, W. Ming, Y. Yao, X. Dai, and Z. Fang, Europhys. Lett. **82**, 67002 (2008).
[6] K. Haule, J. H. Shim, and G. Kotliar, Phys. Rev. Lett. **100**, 226402 (2008).
[7] S. Baroni, A. Dal Corso, S. de Gironcoli, P. Giannozzi, C. Cavazzoni, G. Ballabio, S. Scandolo, G. Chiarotti, P. Focher, A. Pasquarello, K. Laasonen, A. Trave, R. Car, N. Marzari, and A. Kokalj (http://www.quantum-espresso.org).
[8] J. P. Perdew, K. Burke, and M. Ernzerhof, Phys. Rev. Lett. **77**, 3865 (1996).
[9] D. Vanderbilt, Phys. Rev. B **41**, 7892 (1990).
[10] P. Blaha, K. Schwarz, G. K. H. Madsen, D. Kvasnicka, and J. Luitz, *WIEN2K, An Augmented Plane Wave Plus Local Orbits Program for Calculated Crystal Properties* (Karlheinz Schwarz, Technical Universitat Wien, Austria, 2001).